This paper is available on line at http://www.mcponline.org

Stable Isotope Labeling in Zebrafish Allows *in Vivo* Monitoring of Cardiac Morphogenesis*[S]

Anne Konzer§, Aaron Ruhs§, Helene Braun§, Benno Jungblut§, Thomas Braun§, and Marcus Krüger§‡

Quantitative proteomics is an important tool to study biological processes, but so far it has been challenging to apply to zebrafish. Here, we describe a large scale quantitative analysis of the zebrafish proteome using a combination of stable isotope labeling and liquid chromatography-mass spectrometry (LC-MS). Proteins derived from the fully labeled fish were used as a standard to quantify changes during embryonic heart development. LC-MS-assisted analysis of the proteome of activated leukocyte cell adhesion molecule zebrafish morphants revealed a down-regulation of components of the network required for cell adhesion and maintenance of cell shape as well as secondary changes due to arrest of cellular differentiation. Quantitative proteomics in zebrafish using the stable isotope-labeling technique provides an unprecedented resource to study developmental processes in zebrafish. ***Molecular & Cellular Proteomics 12: 10.1074/mcp.M111.015594, 1502–1512, 2013.***

Over the past years, mass spectrometry-based proteomics has been widely used to analyze complex biological samples (1). Although the latest generation of MS instrumentation allows proteome-wide analysis, protein quantitation is still a challenge (2, 3). Metabolic labeling using stable isotopes has been used for almost a century. Today, the most commonly used techniques for relative protein quantification are based on ^{15}N labeling and stable isotope labeling by amino acids in cell culture (SILAC)[1] (4, 5). SILAC was initially developed for cell culture experiments, and recent approaches extended labeling to living organisms, including bacteria (6), yeast (7), flies (8), worms (9), and rodents (10, 11). In addition, several pulsed SILAC (also known as dynamic SILAC) experiments were performed to assess protein dynamics in cell culture and living animals (12–15).

From the §Max-Planck-Institute for Heart and Lung Research, Ludwigstrasse 43, 61231 Bad Nauheim, Germany

Received November 4, 2011, and in revised form, January 14, 2013
Published, MCP Papers in Press, February 14, 2013, DOI 10.1074/mcp.M111.015594

[1] The abbreviations used are: SILAC, stable isotope labeling of amino acids in cell culture; ALCAM, activated leukocyte cell adhesion molecule; GO, Gene Ontology; Lys-6, [$^{13}C_6$]lysine; MO, morpholino oligonucleotide; hpf, hours post fertilization; BisTris, 2-[bis(2-hydroxyethyl)-amino]-2-(hydroxymethyl)propane-1,3-diol; IHC, immunohistochemistry.

The zebrafish (*Danio rerio*) has proved to be an important model organism to study developmental processes. It also serves as a valuable tool to investigate basic pathogenic principles of human diseases such as cardiovascular disorders and tissue regeneration (16). So far, most researchers rely on immunohistochemistry and Western blots for semi-quantitative protein analysis, an approach that is hampered by the paucity of reliable antibodies in zebrafish. Proteomics approaches that depend on two-dimensional gel approaches (17–19) have not gained wide popularity because of issues with workload, reproducibility, and sensitivity (20, 21).

Another approach for protein quantitation is the chemical modification of peptides, and so far several isobaric tagging methods, including ICAT (22), iTRAQ (23), ^{18}O (24), and dimethyl labeling (25), have been proven to be successful methods.

Recently, a quantitative phosphopeptide study based on dimethyl labeling in zebrafish showed the consequences of a morpholino-based kinase knockdown (26). However, each chemical modification bears the risk of nonspecific and incomplete labeling, which complicates mass spectrometric data interpretation.

Alternatively, a metabolic labeling study with stable isotopes was recently performed on adult zebrafish by the administration of a mouse diet containing [$^{13}C_6$]lysine (Lys-6) (27). Feeding adult zebrafish with the Lys-6-containing mouse chow leads to an incorporation rate of 40%, and SILAC labeling was used to investigate protein and tissue turnover.

Here, we have developed a SILAC fish diet made in-house for the complete SILAC labeling of zebrafish. We established a Lys-6-containing diet as a universal fish food for larval and adult zebrafish. The method allows accurate quantitation of large numbers of proteins, and we proved our approach by the analysis of embryonic heart development. In addition, we investigated the consequences of the morpholino-based activated leukocyte cell adhesion molecule (ALCAM) knockdown during development and identified the lipid anchor protein Paralemmin as a down-regulated protein during heart development. Our approach yielded a huge resource of protein expression data for zebrafish development and provided the basis for more refined studies depending on accurate SILAC protein quantification.

EXPERIMENTAL PROCEDURES

Zebrafish Strains and Maintenance—For the experiments, we used the local zebrafish strain "Bad Nauheim (BNA)" and the transgenic line *Tg*(*myl7*:*EGFP-HsHRAS*)^{s883} (28). Adult and embryonic zebrafish were maintained under standard laboratory conditions at 28°C.

Labeling of Zebrafish with [$^{13}C_6$]Lysine—To label adult zebrafish, we developed a heavy diet based on Lys-6-labeled bacteria (*Escherichia coli*), yeast *(Saccharomyces cerevisiae*) (Silantes), SILAC mouse tissue, and SILAC mouse diet (Silantes). The lysine auxotroph *E. coli* DSM1099 was pre-cultured twice overnight in a small volume of M9 medium (Sigma-Aldrich), which was supplemented with 2 g/liter glucose (AppliChem), 0.49 g/liter $MgSO_4 \cdot 7H_2O$ (AppliChem), 0.015 g/liter $CaCl_2 \cdot 2H_2O$ (AppliChem), 2.53 g/liter drop-out amino acids without lysine (Formedium), and 0.05 g/liter [$^{13}C_6$]lysine (Silantes). For large scale culturing, the second pre-culture was diluted 1:100 in supplemented M9 medium and incubated at 30°C until the stationary phase was reached. Finally, Lys-6-labeled bacteria were harvested and freeze-dried using a lyophilizer (Martin Christ freeze dryers).

Lys-6-labeled yeast was purchased from Silantes. As an additional component, we used Lys-6-labeled mouse tissue, including parts from the skeletal muscle, liver, and white adipose tissue. Mouse tissue was chopped, lyophilized, and mixed with fully labeled bacteria, yeast, and SILAC mouse diet. The mixing ratio (dry weight) was 3:2:1:1 mouse tissue/mouse diet/*E. coli*/yeast. To feed larval and juvenile zebrafish, we used a heavy diet based on Lys-6-labeled larvae of the fruit fly *Drosophila melanogaster*, bacteria, yeast, and SILAC mouse diet (Silantes). Cultivation and labeling of flies were performed as described previously (8). Complete labeled fly larvae were lyophilized and mixed according to their dry mass in the following ratio: 2:2:1:1 fly/yeast/*E. coli*/mouse diet. SILAC labeling of all organisms was controlled by protein in solution digestion, and the incorporation rates were calculated as indicated in supplemental Fig. 1. The SILAC labeling of individual proteins is shown in supplemental Table 1.

All zebrafish were fed twice daily with the heavy diet. During the first 6 weeks after hatching, the diet was supplemented with regular nonlabeled fish food (SDS100-200, Special Diets Services). In our study, we used only [$^{13}C_6$]lysine (Lys-6)-labeled organisms because arginine is converted in organisms like yeast and fly (and most likely also in fish) into other amino acids (8, 29). The endoproteinase LysC was used for all protein digestions to get quantifiable peptides with a C-terminal lysine residue. To calculate SILAC incorporation rates, SILAC ratios were set as % SILAC ratio (% label = (SILAC ratio *100)/(SILAC ratio + 1)). For example, a SILAC ratio of 10 would lead to 91% incorporation.

Dissection of Adult Zebrafish Organs and Preparation of Embryonic Zebrafish Hearts—To dissect organs of adult animals, zebrafish were anesthetized with 0.1% ethyl-3-aminobenzoate-methanesulfonic acid salt (Tricaine, Sigma-Aldrich) dissolved in water. Skin and body wall muscle were carefully removed to expose internal organs such as heart, liver, or swim bladder. Organs were removed, quickly rinsed in ice-cold PBS, and frozen in liquid nitrogen. Homozygous embryos of the transgenic line *Tg*(*myl7*:*EGFP-HsHRAS*)^{s883} were anesthetized at 72 and 120 hpf. To isolate heart tissue, embryos were passed through a 1.1-mm needle as described previously (30). Individual GFP-positive ventricles were identified under fluorescent light, collected, and snap-frozen in liquid nitrogen.

Morpholino-mediated Knockdown—Injection of morpholino (MO) antisense oligonucleotide in zebrafish was done as described previously (31). Morpholino targeted to the translation start of ALCAM mRNA (Alc-MO, 5′-TTTATACAGTCCGGCGACAGTCTCA-3′) (GeneTools) was diluted 1:2 with sterile water/phenol red to inject 8 ng into zebrafish embryos at the one- to two-cell stage. To monitor unspecific effects of injections, the standard control morpholino (Ctrl-MO, 5′-CCTCTTACCTCAGTTACAATTTATA-3′) (GeneTools) was used. To assess efficiency of morpholino-mediated knockdown of ALCAM, the phenotype of injected embryos was analyzed by immunohistochemistry at 72 hpf.

Immunohistochemistry—Embryos at 72 hpf were washed gently in PT (0.3% Triton X-100 in PBS, pH 7.3) and fixed in 4% paraformaldehyde/PBS overnight. Whole mount staining was performed in PBT (4% BSA, 0.3% Triton X-100, 0.02% NaN_3 in PBS, pH 7.3) using mouse monoclonal antibody Zn-8 (Hybridoma Bank, 1:10), MF20 (Hybridoma Bank, 1:10), anti-muscle tropomyosin (Hybridoma Bank, 1:10), rabbit antibody anti-Paralemmin (Abcam, 1:50), and Alexa-Fluor-conjugated secondary antibody (Invitrogen) diluted 1:200.

Sample Preparation and Mass Spectrometry—Dissected organs were homogenized in SDS lysis buffer (4% SDS in 100 mM Tris/HCl, pH 7.6) using an Ultra-Turrax (Ika) or a tissue glass Dounce homogenizer (Kontes Glass Co.). For complete lysis, samples were heated for a short time at 95°C. After DNA shearing by sonication, lysates were clarified by centrifugation at 16,000 × *g* for 5 min. Protein concentration was estimated using the DC protein assay (Bio-Rad). To analyze incorporation of Lys-6 in different zebrafish organs, samples were digested in solution as described previously (32). In brief, proteins were precipitated using 4 volumes of ice-cold acetone, and the protein pellet was dissolved in 6 M urea, 2 M thiourea, 10 mM HEPES, pH 8. Next, proteins were reduced with 1 mM dithiothreitol (DTT), alkylated with 5 mM iodoacetamide, and digested with the endopeptidase Lys-C (Wako). Peptides were purified by stop and go extraction tips (33). For large scale studies, lysates were loaded on an SDS-PAGE (NuPAGE 4–12% BisTris gel, Invitrogen), and separated proteins were stained with Colloidal Blue staining kit (Invitrogen). In-gel digestion of evenly sized gel pieces was performed as described previously (34).

Reverse-phase nanoliquid chromatography (LC) was performed by using an Agilent 1200 nanoflow or Proxeon LC system. The LC system was coupled to an LTQ-Orbitrap XL or an LTQ-Orbitrap Velos mass spectrometer (Thermo Fisher Scientific) equipped with a nanoelectrospray source (Proxeon). Chromatographic separation was performed with in-house packed fused silica emitter with an inner diameter of 75 μm. Columns were packed with C_{18}-AQ ReproSil-Pur (3 μm, Dr. Maisch GmbH). Peptide separation was performed with a linear gradient of 5–30% acetonitrile with 0.5% acetic acid for 150 min at a flow rate of 200 nl/min. After eluting from the C18 column, peptides were ionized by electrospray ionization and transferred into the mass spectrometer. Full survey scan spectra (m/z = 300–1650) were acquired in the Orbitrap with a resolution of R = 60,000 after accumulation of 1,000,000 ions. The five most intense peaks from the full MS scan in the LTQ-Orbitrap were isolated (target value of 5000) and fragmented in the linear ion trap using CID (35% normalized collision energy). For LTQ-Orbitrap Velos measurements, the 15 most intense peaks were selected for fragmentation in the linear ion trap.

Raw data were analyzed using the MaxQuant software package (versions 1.2.2.7 and 1.3.0.5) as described previously (35). Database searches were performed with the Andromeda search engine against a zebrafish FASTA database (IPI 3.67, 38,404 entries, and Uniprot release 2012_02, 39,559 entries). SILAC peptide pairs were detected and quantified by MaxQuant using following parameters: LysC as digesting enzyme with a maximum of two missed cleavages, carbamidomethylation of cysteines as fixed modification, oxidation of methionine, and acetylation of the protein N terminus as variable modifications, SILAC amino acid labeling Lys-6. In case of Lys-6 incorporation rate measurements, no missed cleavage was allowed. Maximum mass deviation was set to 7 ppm for the peptide mass and 0.5 Da for MS/MS ions. For identification of peptides and proteins, a false discovery rate of 1% was used, and only peptides with a minimum of six amino acids length were considered for identification.

Only proteins identified with at least two peptides and one unique peptide were included for data analysis. For SILAC analysis, two ratio counts were set as a minimum for quantification. Statistical analysis of data and *t* tests were performed with Perseus (version 1.2.7.0).

Microarrays—A pool of three embryos was collected from wild type and ALCAM-MO-injected zebrafish at 72 hpf for total RNA isolation using the TRIzol reagent (Invitrogen). RNA isolation was performed in triplicate. RNA quality was analyzed using the Bioanalyzer 2100 (Agilent). RNA of wild type ($n = 3$) and ALCAM-MO-injected ($n = 3$) embryos was hybridized to GeneChip Zebrafish Genome Array (Affymetrix). Background correction, normalization, and summarization were conducted with RMA and Bioconductor (23) in R using a custom CDF file from brain array (36) for probe set definitions based on RefSeq identifications. To identify differentially expressed genes between wild type and ALCAM-MO, a linear model was fitted to each gene using the LIMMA package (37). *p* values were calculated based on moderated *t*-statistics and adjusted by the false discovery rate.

Gene Ontology Analysis—Differential protein abundance between developmental stages 72 and 120 hpf was analyzed using Gene Ontology (GO) functional annotations. GO annotation was based on the UniProtKB GOA online. We selected the most representative cellular compartment terms based on mean $\log_2$ SILAC ratios of proteins associated with each GO term to compare abundances between 120 and 72 hpf.

RESULTS

Labeling of Zebrafish with [$^{13}C_6$]Lysine—To generate the SILAC zebrafish, we developed a diet containing Lys-6-labeled proteins from different organisms, including lysine auxotroph bacteria (*E. coli*), yeast (*S. cerevisiae*), and SILAC mouse chow. In addition, the larval diet contains extracts from the fruit fly *D. melanogaster*, and the adult fish diet was supplemented with SILAC mouse tissue (supplemental Table 1). After lyophilization and grinding, we mixed the components according to the presented *pie charts* in Fig. 1*A*. Importantly, we used fully labeled fish (heavy) of the F1 generation and all following generations as an internal standard to quantify proteins from two nonlabeled (light A and light B) zebrafish (Fig. 1*B*). Thus, the direct ratio between the nonlabeled zebrafish can be obtained by dividing the ratios labeled/nonlabeled (also indicated as *heavy/light*) into each other (Fig. 1*C*). The advantage of such a SILAC standard experiment is that the potential effects were excluded due to the diet or other biological variations. Examples for SILAC ratios and their subsequent changes between two nonlabeled fishes are indicated in Fig. 1*D*. First, we fed 2-month-old nonlabeled zebrafish twice a day for 3 months with our SILAC fish diet. After that period, we measured the Lys-6 incorporation rate of protein extracts and observed an average SILAC labeling of up to ~76% in the whole fish. An extension of the Lys-6 administration for up to 11 months results in an average SILAC incorporation of ~85% (Fig. 2*A*). During this feeding period, we have not observed any obvious effects on body weight and locomotive activity of the zebrafish compared with the regular diet ($n = 10$). To achieve a complete labeling, we mated females, prelabeled for 5 months with the SILAC fish diet, with nonlabeled males to breed the F1 generation. The average size after hatching of zebrafish larvae is ~4 mm (38). To produce food particles that are small enough to be eaten by larvae, we enhanced the grinding procedure until the particle size was <1 mm (Fig. 2*B*). In addition to our SILAC diet, once a week we supplemented a nonlabeled regular diet (SDS100, Special Dietary Service) for the first 6 weeks to compensate for missing ingredients (Fig. 2*C*). Not surprisingly, we observed a slight reduction of the initial labeling (−15%). However, this effect was compensated during the next 2 months by feeding the zebrafish the SILAC fish diet exclusively. Under these conditions, we observed an offspring survival rate of ~50% after 6 weeks that is, compared with nonlabeled fish with a regular diet (brine shrimp/*Artemia* and SDS100) and under the same environmental condition, approximately 10% less efficient. Next, we observed a reduced growth curve compared with fish that are fed the regular nonlabeled diet (Fig. 2*D*). Although smaller in size, the number of eggs from SILAC-labeled females is comparable with nonlabeled females. Taken together, we are aware that our diet has effects on the zebrafish development, but fully labeled zebrafish of the F1 generation and all subsequent F2- and F3-tested generations produced only slightly reduced numbers of fertile eggs, which allows us to maintain a SILAC fish colony as a source for an internal protein standards.

Fully Labeled SILAC Zebrafish of the F1 Generation—Full tissue labeling was demonstrated by the analysis of several tissues, including heart, brain, skeletal muscle, and gills from 3-month-old F1 zebrafish (Fig. 2*E* and supplemental Fig. 2). Here, we observed an average labeling of >95% for all organs tested, and as an example for a stable protein, we detected for the lens protein crystalline β a Lys-6 incorporation rate of 96% (Fig. 2*F* and supplemental Table 2). To test our SILAC-based quantitation method in fish, we mixed heart tissue from labeled zebrafish (H_{SILAC}) with nonlabeled zebrafish (H_{Light}) and performed technical triplicates (supplemental Fig. 3). Because we were using SILAC tissue as an internal standard, ratios of ratios were calculated (supplemental Table S3). Direct comparison of SILAC ratios between replicates revealed Pearson correlations (*r*) ranging from 0.93 to 0.96 and a mean coefficient of variation of 1.4%, indicating only minor technical variability (supplemental Fig. 3*A*). Next, we mixed labeled heart protein lysate into three unlabeled hearts ($H_{Light1-3}$) to investigate biological variations between different individuals ($n = 3$). We calculated Pearson correlations (*r*) ranging from 0.79 to 0.85 and the mean coefficient of variation of 4.5% suggesting that SILAC quantification in zebrafish provides the same statistical accuracy as demonstrated for cell culture and other living animals (39).

Quantitative Proteomics of Heart Development Using Fully Labeled Zebrafish—To demonstrate the value of our method for large scale quantitative analysis of early zebrafish embryonic development, we compared embryonic zebrafish hearts at 72 and 120 h after fertilization (hpf). We employed *Tg*(*myl7*:*EGFP-HsHRAS*)^{s883} zebrafish, which express the green fluorescence protein (GFP) under the control of the cardiac my-

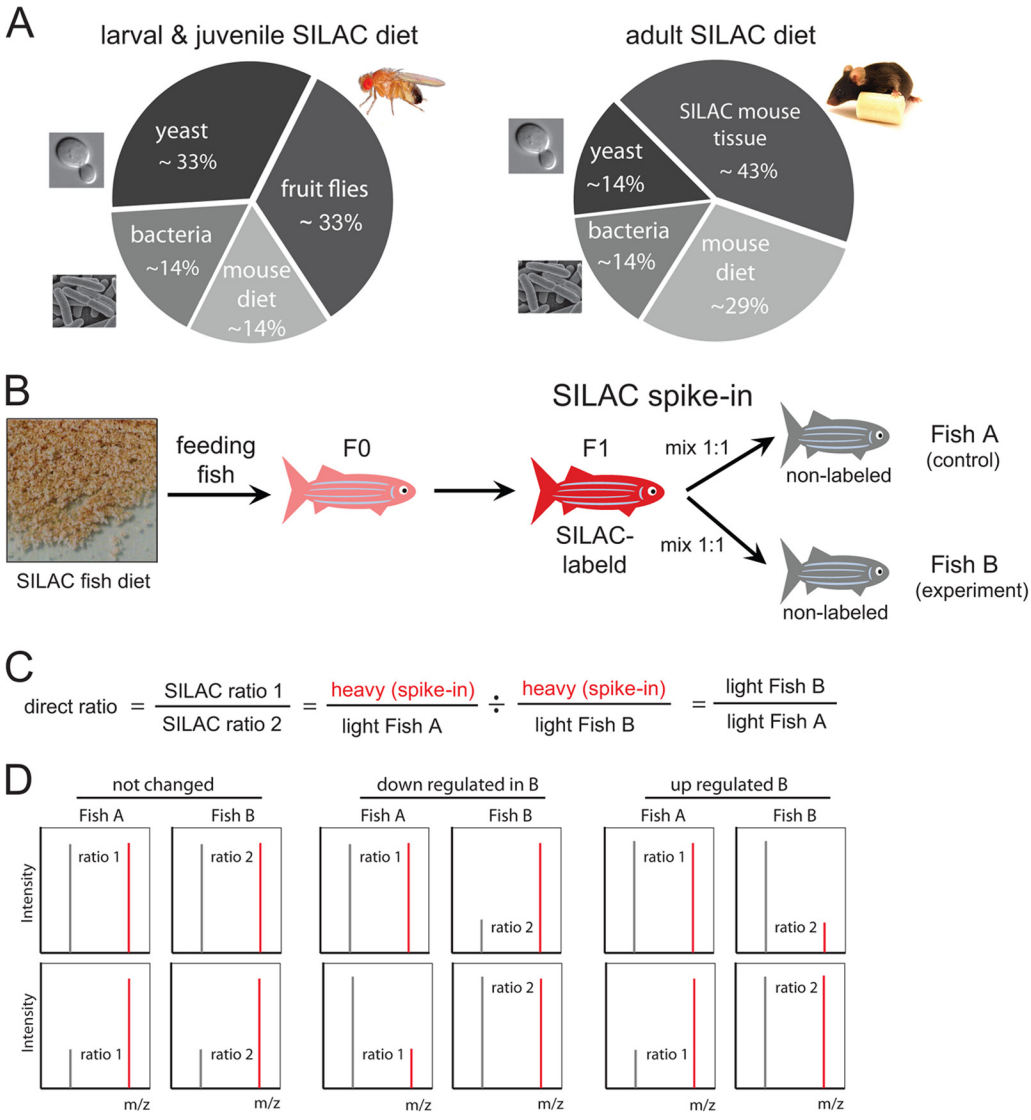

FIG. 1. **Development of the SILAC fish diet for metabolic labeling of *D. rerio*.** *A,* In-house-developed SILAC diet for adult zebrafish consists of heavy labeled cells of *E. coli*, *S. cerevisiae*, mouse tissue, and SILAC mouse diet. The larval SILAC diet is based on Lys-6-labeled larvae of *D. melanogaster* and cells of *E. coli*, *S. cerevisiae,* and SILAC mouse diet. Mixing ratios are based on dry weight. *B,* all components were grinded to create a fine powder that can be consumed by the zebrafish. *Red colored fish* indicates complete SILAC labeling. *C,* SILAC fish can be used as an internal standard for protein quantitation to compare two nonlabeled zebrafish (*Fish A* and *B*). By calculating direct ratios out of SILAC ratios, protein expression levels between nonlabeled zebrafish can be compared. *D,* examples of SILAC pairs and the subsequent regulation between nonlabeled (*black peak*) samples. The SILAC peak is indicated in *red*.

osin light chain 2 (myl7) promoter to facilitate isolation of early embryonic heart tissue (Fig. 3*A*) (28). Approximately 400 GFP-positive hearts were isolated yielding ~20 μg of protein extract from both developmental stages. Total protein lysates from 72 hpf SILAC embryos were used as labeled protein standard and were combined with equal amounts of protein from unlabeled heart tissue of both developmental stages to perform a quantitative SILAC experiment (Fig. 3*B*). Based on biological triplicates ($n = 3$), we calculated the median SILAC ratio and quantified 1955 proteins at both time points at a false discovery rate of 1%. 327 proteins showed a significant ($p < 0.05$) fold change $\geq$2 after 120 hpf compared with 72 hpf. GO analysis of regulated candidates in relation to all identified proteins revealed a clear over-representation of GO terms belonging to calcium ion transport, cellular respiration, and heart morphogenesis (supplemental Fig. 4 and Table 4). An exemplary SILAC pair for tropomyosin 2 is shown in Fig. 3*D*. Our findings indicate progressive differentiation and maturation of subcellular structures of cardiomyocytes during heart development such as the contractile apparatus and the sarcoplasmic reticulum (Fig. 3*E*). Conversely, we identified 124 proteins that were >2-fold down-regulated ($p < 0.05$) during the course of development. These proteins are highly diverse, and enrichments of GO categories are detectable only for

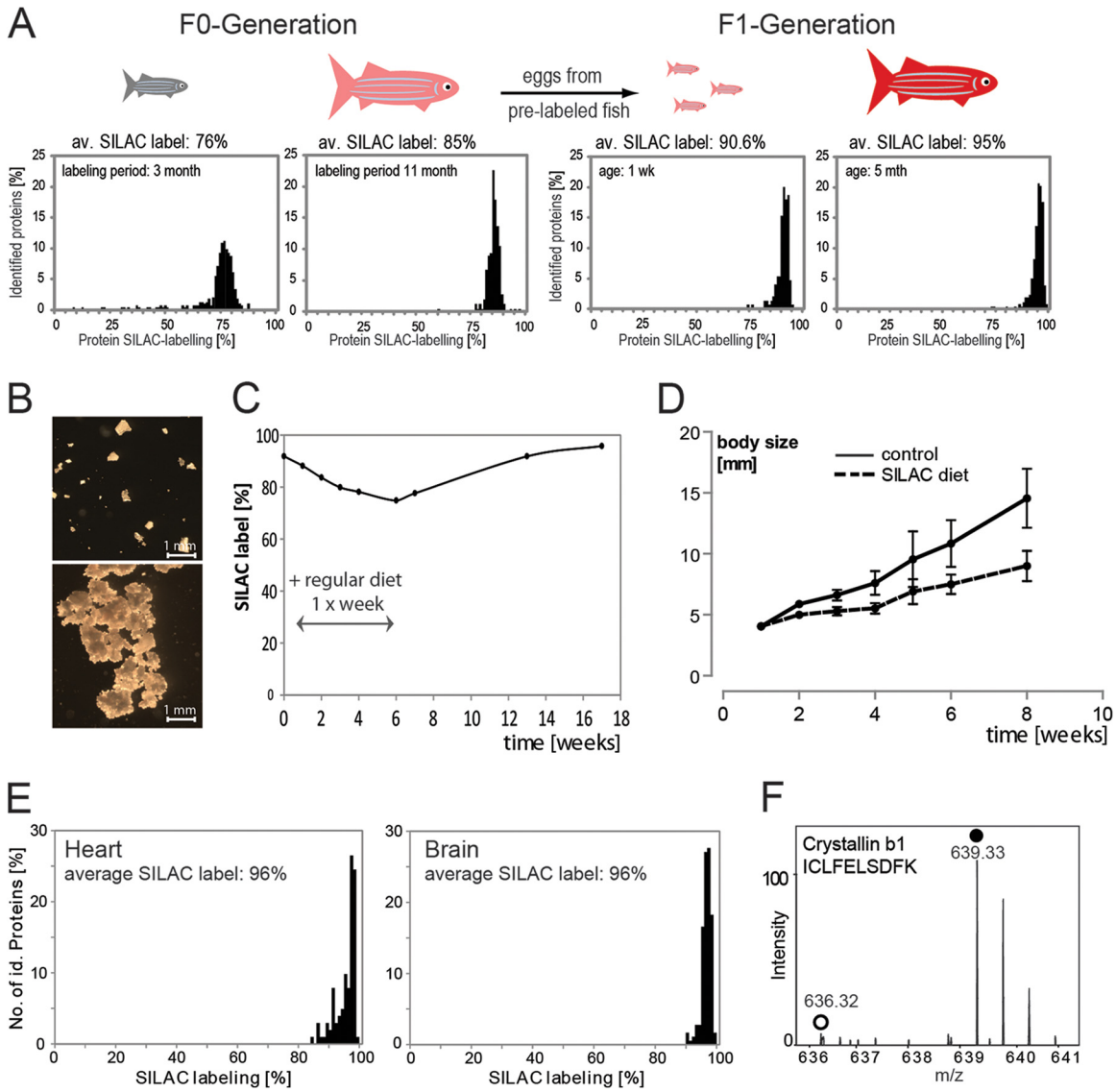

FIG. 2. **Full SILAC labeling of F1 generation fish.** *A,* nonlabeled adult (age 2 months) wild type zebrafish were fed with Lys-6 diet for 3 and 11 months. Incorporation rates were plotted against the relative number of identified proteins. The analysis contains ~200 proteins per plot. The analysis of 1-week-old larvae revealed an average labeling of ~90%. The SILAC incorporation rates of 95% was observed after 5 months of the F1 generation (*A, right histogram*). *B,* SILAC diet for larvae and adult zebrafish differs in their composition and particle size. *C,* administration of SILAC diet supplemented with regular nonlabeled food. The *graph* shows the relative SILAC labeling in percent plotted against the time in weeks. *Arrows* indicate the time period with the nonlabeled diet. *D,* growth of zebrafish embryos fed with regular diet (Special Diets Services, *black curve*) and SILAC diet (*dashed curve*) over a time course of 8 weeks after fertilization. Each time point represents 10 embryos ($n = 10$). The average body size of SILAC embryos is 9 mm (+/−2 mm) at 8 weeks compared to 14.6 mm (+/−3 mm) with embryos administered a regular diet. *E,* relative numbers of proteins with specific Lys-6 incorporation rates are shown for heart ($n = 424$) and brain ($n = 729$) of adult zebrafish from the F1 generation to confirm complete Lys-6 incorporation. *F,* SILAC pair of a selected crystallin peptide indicates ~95% labeling.

integrin signaling and lipoprotein metabolism (supplemental Fig. 4). We also identified strong expression of proliferating cell nuclear antigen at the early developmental stage (Fig. 3*D*), which reflects strong morphometric activity and cardiomyocyte proliferation at 72 hpf. Taken together, the *in vivo* SILAC approach of whole Lys-6-labeled embryos enables accurate protein quantification of developing zebrafish hearts.

Loss of ALCAM Leads to Changes in the Protein Network Responsible for Cell Adhesion and Cell Shape—One of the advantages of the zebrafish system is the straightforward generation of loss-of-function morphants. To evaluate whether SILAC-based proteomics might be applied for analysis of loss-of-function morphants, we knocked down the cell adhesion protein ALCAM. ALCAM plays a crucial role in the

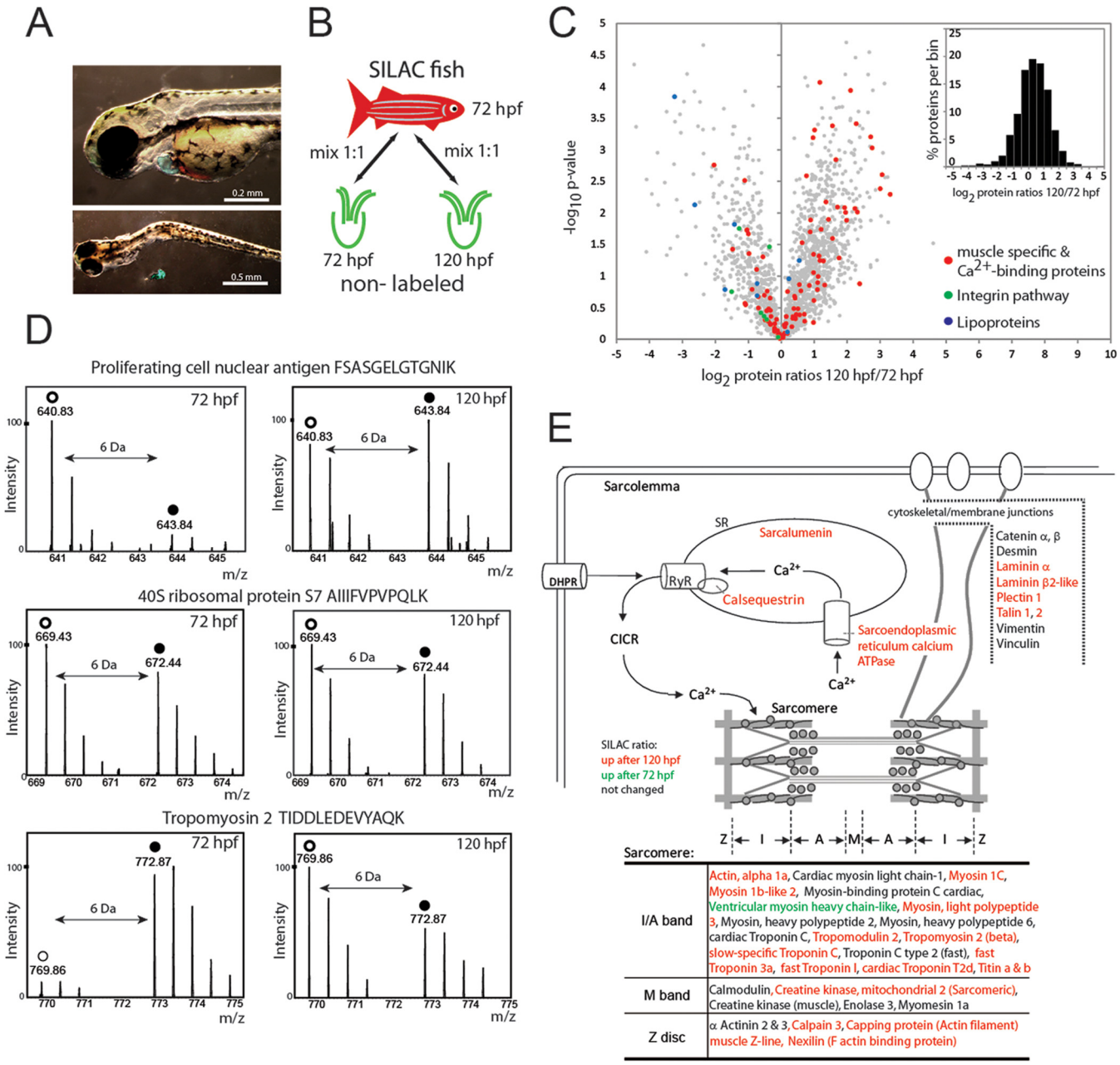

FIG. 3. **Analysis of cardiac development in zebrafish.** *A*, embryonic hearts were isolated at 72 and 120 hpf using the cmlc2-GFP reporter zebrafish strain. A single isolated *green heart* is shown in the *lower panel*. *B*, Lys-6-labeled tissue from 72-hpf embryos were used as a standard to quantify hearts from two nonlabeled developmental stages. *C*, volcano plot and histogram of 1955 quantified proteins between nonlabeled 72- and 120-hpf embryos. 327 proteins out of 1955 proteins are up-regulated (≥2-fold change, $p < 0.05$) at 120 hpf, and 124 proteins are enriched at 72 hpf. *D*, selected MS spectra of proteins enriched at 72 hpf (proliferating cell nuclear antigen), with no regulation (40 S ribosomal protein S7), and with higher abundance at 120 hpf (tropomyosin 2). *E*, pathway analysis shows an up-regulation at 120 hpf for several proteins, which are related to muscle contraction and calcium homeostasis.

morphogenesis of eye, cartilage, heart, and swim bladder (40, 41) in fish and is strongly expressed in activated leukocytes in mammals. Injection of morpholino (MO) antisense oligonucleotides efficiently blocked translation of ALCAM mRNA as indicated by IHC staining using an ALCAM antibody (Zn-8) and mass spectrometric detection of ALCAM peptides (Fig. 4, *A* and *B*). ALCAM morphants were smaller in size and showed severe malformations of the heart.

To analyze effects of the loss of ALCAM on proteome composition, we pooled 10 embryos of nonlabeled control (non-MO-injected) and ALCAM-MO-injected 72-hpf zebrafish embryos and mixed these samples with equal amounts of

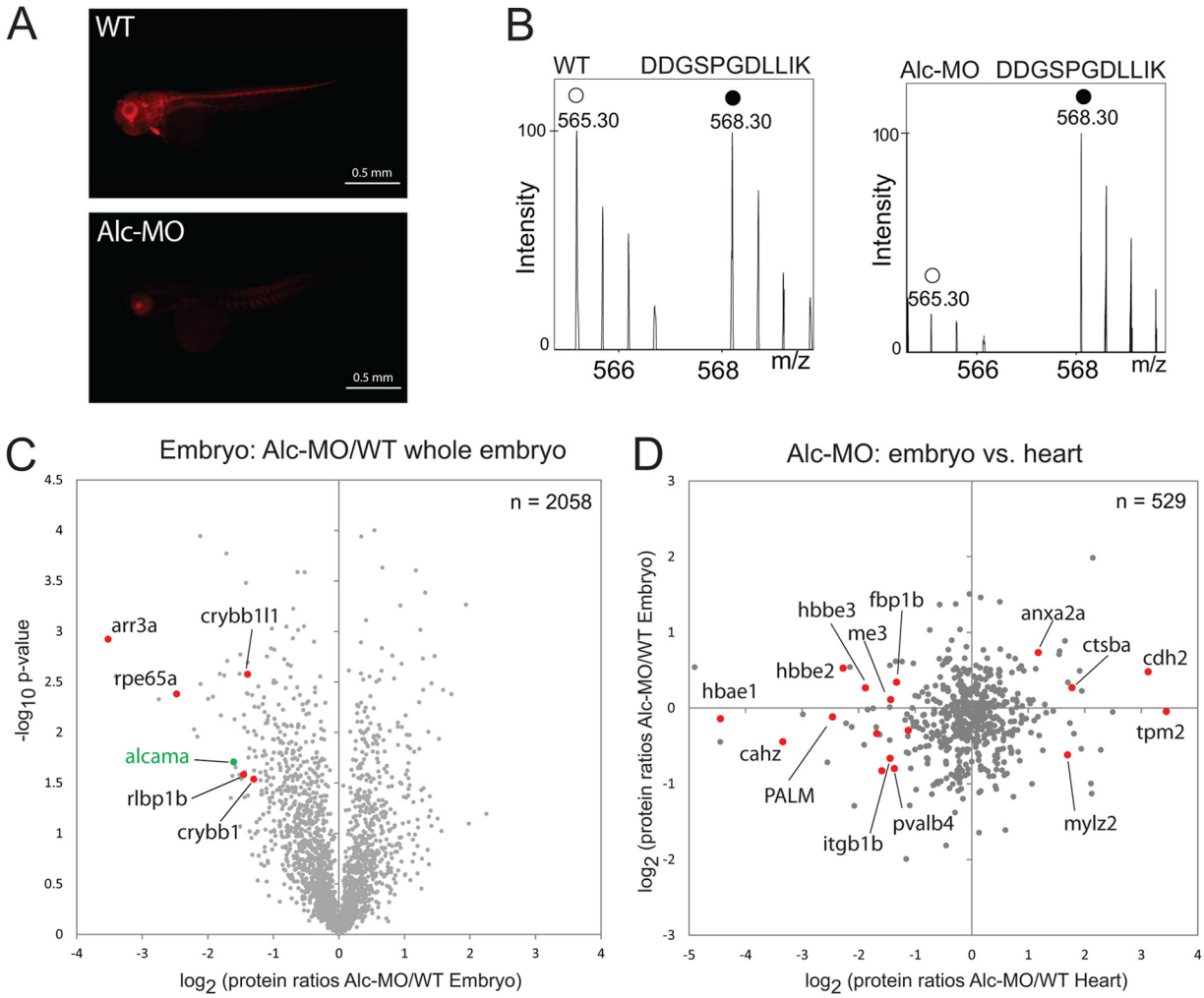

FIG. 4. **Knockdown of ALCAM reveals defective retina and heart development.** *A*, decreased expression of ALCAM was confirmed by whole mount staining with the ALCAM antibody Zn-8. *B*, selected MS spectra of an ALCAM-derived peptide. *C*, direct ratios between nonlabeled ALCAM morphants (*Alc-MO*) and non-MO-injected embryos at 72 hpf are plotted against negative logarithmic *p* values. 2058 proteins were quantified. Selected proteins with more than a 2-fold change are shown in *red*. *D*, comparison of SILAC ratios derived from whole embryos (*Alc-MO/WT*) and isolated hearts. Colored proteins are regulated only in the heart dataset.

protein from 72-hpf fully labeled zebrafish embryos. Sample preparation, in-gel digestion, and mass spectrometric analyses were performed in biological triplicates ($n = 3$). Data analysis with MaxQuant and Perseus revealed 2058 quantified proteins (Fig. 4*C* and supplemental Table 5). 81 proteins (~4%) showed a significant ($p < 0.05$) 2-fold down-regulation in the absence of ALCAM. Our analysis confirmed a strong down-regulation (~3-fold) of ALCAM as a result of the translational arrest. Furthermore, we detected down-regulation of several proteins located in the retina ganglion cell layer, including arrestin-3 and the retinal pigment epithelium-specific protein, which most likely reflect arrest of retina ganglion cell layer differentiation in ALCAM morphants (40).

Because the use of whole embryo extracts might obscure tissue-specific changes, we again took advantage of the *Tg*(*myl7*:*EGFP-HRAS*)^{s883} reporter zebrafish strain and repeated the quantitative proteome analysis using a pool of 100 isolated hearts and performed two biological replicates ($n = 2$). We used 10 μg of starting material (5 μg of heavy + 5 μg of light), and we quantified 925 proteins in wild type and ALCAM-depleted hearts at 72 hpf, including 58 proteins that were significantly regulated ($p < 0.05$). In total, we detected 70 proteins that were down-regulated with a fold change of >2 (supplemental Table 5). Among others, we found reduced protein levels of the integrin receptor β, the Ras-like protein Rac1a, and Paralemmin, which are important regulators for cell adhesion, cytoskeletal reorganization, and cell shape maintenance (42, 43). Comparison of the proteomics dataset of whole fish embryos with the heart-specific dataset identified several proteins, including carbonic anhydrase, integrin β, Parvalbumin-4, and Paralemmin, which were only down-regulated in the heart (Fig. 4*D*). The expression of myosin heavy chains (MF20 antibody), tropomyosin, and Paralemmin were confirmed by IHC staining (Fig. 5).

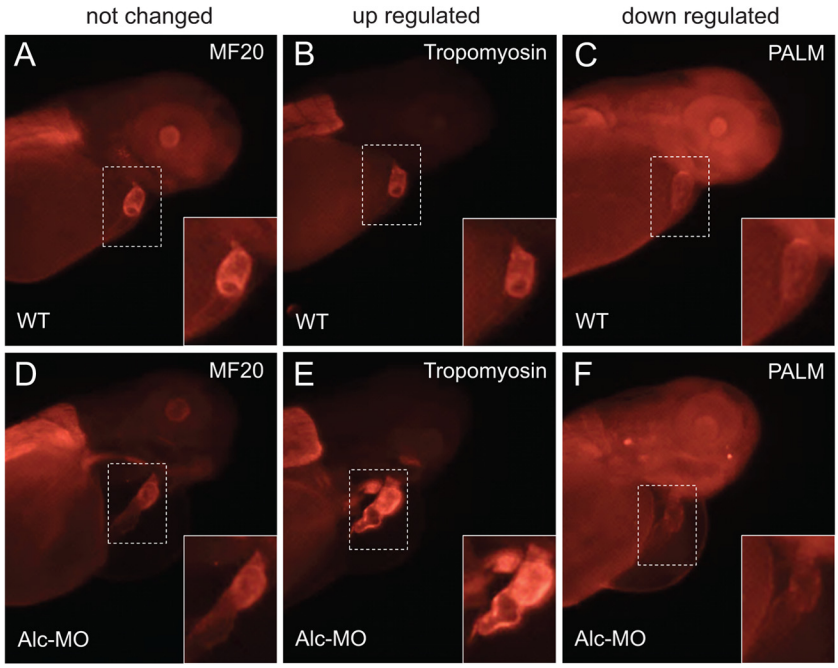

FIG. 5. **IHC staining confirms regulated candidates in ALCAM morphants.** Panels show wild type (*WT*) (*A–C*) and ALCAM-MO (*Alc-MO*) (*D–F*)-injected embryos in lateral views, with anterior to the *right* and dorsal to the *top*; the higher magnifications of hearts are shown in the *insets*. *A* and *D,* controls were performed with an MF20 antibody that is directed against myosin heavy chain. *B* and *E,* staining with an antibody against tropomyosin reveals higher expression in hearts of Alc-MO. *C* and *F,* Paralemmin antibody staining indicates a reduced expression.

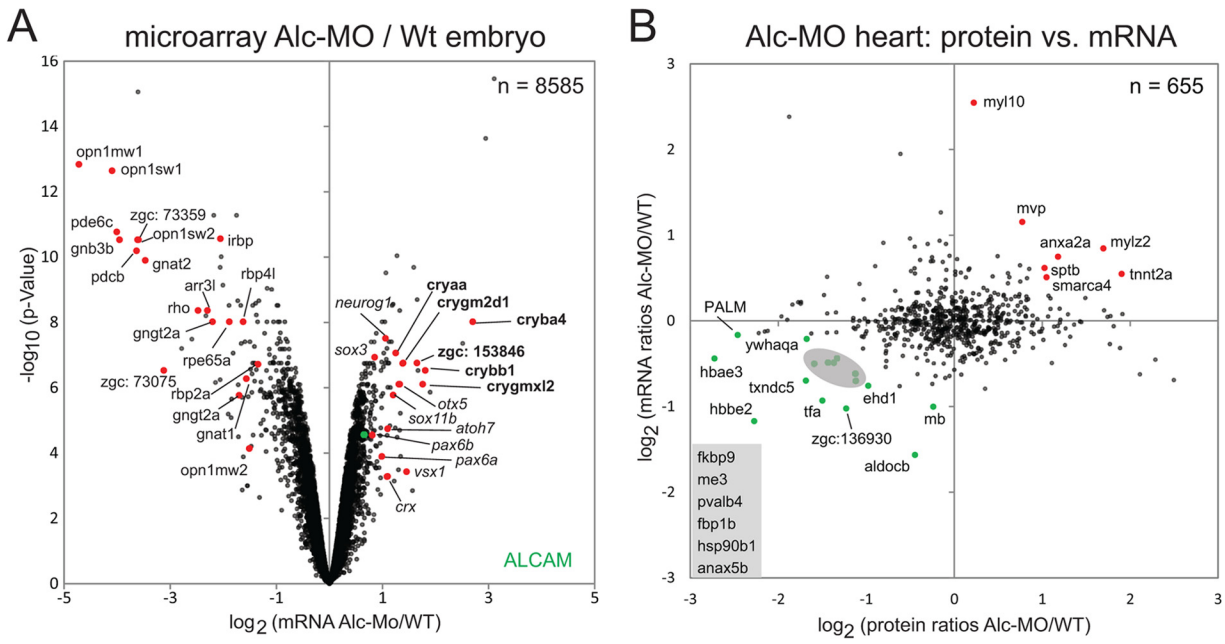

FIG. 6. **Gene expression analysis of ALCAM morphants.** *A,* gene expression analysis using Affymetrix zebrafish microarrays was performed with wild type embryos ($n = 3$) and Alc-MO ($n = 3$). Regulated genes (fold change >2 and $p < 0.05$) are shown in *red*. *B,* overall correlation of transcriptome and proteome derived from isolated hearts (*Alc-MO/WT*). Colored candidates are regulated on mRNA and protein level.

To also gain insight into the changes at the transcript level, we performed an Affymetrix DNA microarray analysis of control and ALCAM morphants based on biological triplicates ($n = 3$) (Fig. 6*A*). We identified 8585 genes with a Refseq identifier using the brain array software tool (36). 102 genes (1.2%) showed a 2-fold down-regulation (p value <0.05), including several retina proteins (photoreceptors and several subunits of heterotrimeric guanine nucleotide-binding proteins (G proteins)), which partially confirmed the results of the proteomics analysis (supplemental Table 5). No changes in ALCAM mRNA levels were seen because we used a morpholino targeting post-spliced mRNA. Interestingly, several neuronal transcription factors, including neurogenin-1, Atoh 7, and Sox-3, were up-regulated suggesting increased numbers of immature proliferating neurons and delayed development of the retina in ALCAM morphants. Correlation of proteomics

and transcriptomics data yielded a relatively weak Pearson correlation of 0.37 in the group of down-regulated molecules. In total, 1589 genes (~76% of all detected proteins) were detected both on the protein and mRNA levels (supplemental Fig. 5). We next performed an Affymetrix DNA microarray analysis of isolated ALCAM and control morphant hearts resulting in the detection of 8585 expressed genes (Fig. 6*B*). Nine molecules showed a down-regulation with a fold change of >1.5 on both mRNA and protein levels. 92 molecules were only regulated on the protein level but not on the mRNA level, and nine genes were down-regulated at the mRNA but not on the protein level. Pearson correlation of all heart-specific proteins and mRNAs was 0.09 (Fig. 6*B* and supplemental Table 5). The relatively weak concordance of protein and mRNA datasets illustrates the benefit of a careful proteomic analysis of morphants, because numerous molecules that changed expression after inactivation of ALCAM would not have been detected by a DNA microarray analysis alone.

DISCUSSION

The zebrafish as a model system has a number of distinctive features, including the ready access to all developmental stages. The optical clarity of embryos and larvae allows direct imaging of emerging pathological changes. Moreover, large scale screening approaches are on hand, which are difficult to afford in mammals. Another advantage is the availability of morpholino-based transient *in vivo* assays permitting rapid access to functional studies, although this approach is restricted to early developmental stages.

Conversely, protein analysis has not been a major strength of the zebrafish system mostly due to the paucity of antibody reagents available, the lack of robust cell and tissue culture systems, and the limited amount of material available for biochemical analysis (44). New techniques and instrumentations, however, are beginning to overcome these restrictions. Here, we presented a mass spectrometric approach based on *in vivo* incorporation of [$^{13}C_6$]lysine into zebrafish proteins. Labeling of zebrafish was based on a general SILAC-based fish diet, which should be easily adaptable to other fish species such as the Japanese rice fish Medaka (*Oryzias latipes*).

Pathological tissue remodeling and injuries as well as tissue repair and regeneration involve multiple regulatory levels, including changes in gene transcription, mRNA stability, and translation and alterations of proteins stability and modification.

As a proof-of-principle, we used proteins isolated from fully labeled SILAC zebrafish of the F1 generation as an internal protein standard to analyze embryonic zebrafish heart development. Comparison of two developmental stages during early heart formation unveiled multiple changes in the protein repertoire of cardiomyocytes during day 3 and day 5 of zebrafish development, which reflected the ongoing differentiation and functional maturation of the heart. Up-regulation of differentiation markers during development was accompanied by down-regulation of proteins involved in the integrin signaling pathway. It will be interesting to compare this dataset to available data from early mouse and human hearts to characterize the core program of heart development shared by all vertebrates.

Zebrafish embryos are particularly amendable to transient *in vivo* studies using morpholino-based gene knockdown strategies. Morpholino-mediated suppression of translation starts to lose its efficiency within 50 h after injection, which restricts the window for analysis to early embryonic stages. So far, the limited amount of material that can be obtained from embryonic fish has made analysis of proteins difficult. Our newly developed SILAC-based mass spectrometry approach, however, allowed us to perform a proteome-wide analysis of ALCAM morphants obtained 72 h after injection of antisense morpholinos targeting the translational start site. The sensitivity of the technique was sufficient to focus on a particular organ of interest, in our case the embryonic heart, thereby enhancing the depth of analysis.

ALCAM is a cell adhesion gene, which is expressed in activated leukocytes, in hematopoietic cells, and in cancer cells (45), as well as in developing eyes and hearts (46). It is assumed that ALCAM provides a link between extracellular receptors and the intracellular cytoskeleton. Moreover, ALCAM is involved in the regulation of the cell shape (42). In line with the proposed connection of the ALCAM-mediated adhesion with the integrin pathway and small GTPases, we found reduced protein levels of the integrin receptor β, the Ras-like protein Rac1a, and Paralemmin. All these proteins are important regulators of cell adhesion, cytoskeletal reorganization, and cell shape maintenance (42, 43) emphasizing the role of ALCAM in these processes. At present, we do not know the exact reason for the down-regulation of integrin receptor β, Rac1a, and Paralemmin. Most likely, depletion of ALCAM leads to a disturbed cross-talk between adhesion proteins and the cytoskeleton and subsequently to a down-regulation of other components of the machinery that mediates interaction of the cell adhesion apparatus and cytoskeleton. Additional studies, such as SILAC-based screening for proteins that interact with ALCAM will allow more detailed insights into the function of ALCAM during early heart formation. Surprisingly, comparison of proteome and transcriptome data of ALCAM-depleted fish embryos revealed only a weak correlation between changes in mRNA and protein levels. In principle, it is possible that the rather weak overlap is due to biological differences caused by post-transcriptional and post-translational mechanisms such as micro RNA-based mechanisms or changes in protein stability. It seems unlikely, however, that all differences can be attributed to biological phenomena. In fact, the DNA microarrays, which are currently available for analysis of zebrafish, suffer from a number of shortcomings, including imperfect annotations, relatively low number of probe sets, incomplete coverage of different isoforms, and quality problems with some microarrays. These deficiencies were particularly evident when we detected nu-

merous proteins by our MS approach, which yielded no signals on the microarrays indicating faulty probe sets. In addition, we monitored multiple proteins, which were not covered by probe sets on the microarrays. Despite these inconsistencies, we detected a number of molecules, which showed the same type of regulation by mass spectrometry and microarray analysis supporting a function of ALCAM in eye and heart development. We reasoned that our quantitative proteomics approach provides a useful method to study proteome-wide changes in zebrafish. The recently discovered zinc finger nucleases and the transcription activator-like effector proteins are excellent tools to generate locus-specific mutations in the zebrafish (47, 48). Those zebrafish mutants can be readily analyzed with our SILAC-labeled zebrafish. In addition, our approach can be adapted to other large scale peptide and protein quantification experiments in zebrafish and other related species.

Dataset 1 contains RAW files derived from the heart development study. Dataset 2 contains all RAW data obtained from the ALCAM morpholino knockdown experiments. All RAW files can be downloaded from the Tranche Server. Hash codes are listed in supplemental Table S6.

Acknowledgments—We thank Sylvia Jeratsch for excellent technical assistance and Monika Müller-Boche for excellent animal care. We thank Pascal Gellert, Mario Looso, and Matthew Wheeler for help and discussions.

* This work was supported by the Max-Planck-Society and the Excellence Initiative "Cardiopulmonary System," the University of Giessen-Marburg Lung Center, and the Cell and Gene Therapy Center supported by the Hessian Ministry for Science and the Arts.

S This article contains supplemental material.

‡ To whom correspondence should be addressed. Tel.: 496032-705-1760; E-mail: marcus.krueger@mpi-bn.mpg.de.

REFERENCES

1. Walther, T. C., and Mann, M. (2010) Mass spectrometry-based proteomics in cell biology. *J. Cell Biol.* **190**, 491–500
2. Mann, M., and Kelleher, N. L. (2008) Precision proteomics: the case for high resolution and high mass accuracy. *Proc. Natl. Acad. Sci. U.S.A.* **105,** 18132–18138
3. Elliott, M. H., Smith, D. S., Parker, C. E., and Borchers, C. (2009) Current trends in quantitative proteomics. *J. Mass Spectrom.* **44,** 1637–1660
4. Schoenheimer, R., and Rittenberg, D. (1935) Deuterium as an indicator in the study of intermediary metabolism. *Science* **82,** 156–157
5. Ong, S. E., Blagoev, B., Kratchmarova, I., Kristensen, D. B., Steen, H., Pandey, A., and Mann, M. (2002) Stable isotope labeling by amino acids in cell culture, SILAC, as a simple and accurate approach to expression proteomics. *Mol. Cell. Proteomics* **1,** 376–386
6. Soufi, B., Kumar, C., Gnad, F., Mann, M., Mijakovic, I., and Macek, B. (2010) Stable isotope labeling by amino acids in cell culture (SILAC) applied to quantitative proteomics of *Bacillus subtilis*. *J. Proteome Res.* **9,** 3638–3646
7. Gruhler, A., Olsen, J. V., Mohammed, S., Mortensen, P., Faergeman, N. J., Mann, M., and Jensen, O. N. (2005) Quantitative phosphoproteomics applied to the yeast pheromone signaling pathway. *Mol. Cell. Proteomics* **4,** 310–327
8. Sury, M. D., Chen, J. X., and Selbach, M. (2010) The SILAC fly allows for accurate protein quantification *in vivo*. *Mol. Cell. Proteomics* **9,** 2173–2183
9. Larance, M., Bailly, A. P., Pourkarimi, E., Hay, R. T., Buchanan, G., Coulthurst, S., Xirodimas, D. P., Gartner, A., and Lamond, A. I. (2011) Stable isotope labeling with amino acids in nematodes. *Nat. Methods* **8,** 849–851
10. McClatchy, D. B., Dong, M. Q., Wu, C. C., Venable, J. D., and Yates, J. R., 3rd (2007) ^{15}N metabolic labeling of mammalian tissue with slow protein turnover. *J. Proteome Res.* **6**, 2005–2010
11. Krüger, M., Moser, M., Ussar, S., Thievessen, I., Luber, C. A., Forner, F., Schmidt, S., Zanivan, S., Fässler, R., and Mann, M. (2008) SILAC mouse for quantitative proteomics uncovers kindlin-3 as an essential factor for red blood cell function. *Cell* **134,** 353–364
12. Doherty, M. K., Whitehead, C., McCormack, H., Gaskell, S. J., and Beynon, R. J. (2005) Proteome dynamics in complex organisms: using stable isotopes to monitor individual protein turnover rates. *Proteomics* **5,** 522–533
13. Doherty, M. K., Hammond, D. E., Clague, M. J., Gaskell, S. J., and Beynon, R. J. (2009) Turnover of the human proteome: determination of protein intracellular stability by dynamic SILAC. *J. Proteome Res.* **8,** 104–112
14. Looso, M., Borchardt, T., Krüger, M., and Braun, T. (2010) Advanced identification of proteins in uncharacterized proteomes by pulsed *in vivo* stable isotope labeling-based mass spectrometry. *Mol. Cell. Proteomics* **9,** 1157–1166
15. Schwanhäusser, B., Gossen, M., Dittmar, G., and Selbach, M. (2009) Global analysis of cellular protein translation by pulsed SILAC. *Proteomics* **9,** 205–209
16. Siccardi, A. J., 3rd, Garris, H. W., Jones, W. T., Moseley, D. B., D'Abramo, L. R., and Watts, S. A. (2009) Growth and survival of zebrafish (*Danio rerio*) fed different commercial and laboratory diets. *Zebrafish* **6,** 275–280
17. Lucitt, M. B., Price, T. S., Pizarro, A., Wu, W., Yocum, A. K., Seiler, C., Pack, M. A., Blair, I. A., Fitzgerald, G. A., and Grosser, T. (2008) Analysis of the zebrafish proteome during embryonic development. *Mol. Cell. Proteomics* **7,** 981–994
18. Singh, S. K., Meena Lakshmi, M. G., Saxena, S., Swamy, C. V., and Idris, M. M. (2011) Proteome profile of zebrafish caudal fin based on one-dimensional gel electrophoresis LCMS/MS and two-dimensional gel electrophoresis MALDI MS/MS analysis. *J. Sep. Sci.,* **34,** 225–232
19. De Wit, M., Keil, D., van der Ven, K., Vandamme, S., Witters, E., and De Coen, W. (2010) An integrated transcriptomic and proteomic approach characterizing estrogenic and metabolic effects of 17-α-ethinylestradiol in zebrafish (*Danio rerio*). *Gen. Comp. Endocrinol.* **167**, 190–201
20. Gygi, S. P., Rist, B., and Aebersold, R. (2000) Measuring gene expression by quantitative proteome analysis. *Curr. Opin. Biotechnol.* **11,** 396–401
21. Petrak, J., Ivanek, R., Toman, O., Cmejla, R., Cmejlova, J., Vyoral, D., Zivny, J., and Vulpe, C. D. (2008) Deja vu in proteomics. A hit parade of repeatedly identified differentially expressed proteins. *Proteomics* **8,** 1744–1749
22. Smolka, M. B., Zhou, H., Purkayastha, S., and Aebersold, R. (2001) Optimization of the isotope-coded affinity tag-labeling procedure for quantitative proteome analysis. *Anal. Biochem.* **297,** 25–31
23. Gentleman, R. C., Carey, V. J., Bates, D. M., Bolstad, B., Dettling, M., Dudoit, S., Ellis, B., Gautier, L., Ge, Y., Gentry, J., Hornik, K., Hothorn, T., Huber, W., Iacus, S., Irizarry, R., Leisch, F., Li, C., Maechler, M., Rossini, A. J., Sawitzki, G., Smith, C., Smyth, G., Tierney, L., Yang, J. Y., and Zhang, J. (2004) Bioconductor: open software development for computational biology and bioinformatics. *Genome Biol.* **5,** R80
24. Miyagi, M., and Rao, K. C. (2007) Proteolytic ^{18}O-labeling strategies for quantitative proteomics. *Mass Spectrom. Rev.* **26,** 121–136
25. Kovanich, D., Cappadona, S., Raijmakers, R., Mohammed, S., Scholten, A., and Heck, A. J. (2012) Applications of stable isotope dimethyl labeling in quantitative proteomics. *Anal. Bioanal. Chem.* **404,** 991–1009
26. Lemeer, S., Jopling, C., Naji, F., Ruijtenbeek, R., Slijper, M., Heck, A. J., and den Hertog, J. (2007) Protein-tyrosine kinase activity profiling in knockdown zebrafish embryos. *PloS One* **2,** e581
27. Westman-Brinkmalm, A., Abramsson, A., Pannee, J., Gang, C., Gustavsson, M. K., von Otter, M., Blennow, K., Brinkmalm, G., Heumann, H., and Zetterberg, H. (2011) SILAC zebrafish for quantitative analysis of protein turnover and tissue regeneration. *J. Proteomics* **75,** 425–434
28. D'Amico, L., Scott, I. C., Jungblut, B., and Stainier, D. Y. (2007) A mutation in zebrafish hmgcr1b reveals a role for isoprenoids in vertebrate heart-tube formation. *Curr. Biol.* **17,** 252–259
29. Bicho, C. C., de Lima Alves, F., Chen, Z. A., Rappsilber, J., and Sawin, K. E. (2010) A genetic engineering solution to the "arginine conversion problem" in stable isotope labeling by amino acids in cell culture (SILAC). *Mol.*

Cell. Proteomics **9,** 1567–1577
30. Burns, C. G., and MacRae, C. A. (2006) Purification of hearts from zebrafish embryos. *BioTechniques* **40**, 274
31. Nasevicius, A., and Ekker, S. C. (2000) Effective targeted gene "knockdown" in zebrafish. *Nat. Genet.* **26,** 216–220
32. Andersen, J. S., Lam, Y. W., Leung, A. K., Ong, S. E., Lyon, C. E., Lamond, A. I., and Mann, M. (2005) Nucleolar proteome dynamics. *Nature* **433,** 77–83
33. Rappsilber, J., Ishihama, Y., and Mann, M. (2003) Stop and go extraction tips for matrix-assisted laser desorption/ionization, nanoelectrospray, and LC/MS sample pretreatment in proteomics. *Anal. Chem.* **75,** 663–670
34. Shevchenko, A., Tomas, H., Havlis, J., Olsen, J. V., and Mann, M. (2006) In-gel digestion for mass spectrometric characterization of proteins and proteomes. *Nat. Protoc.* **1,** 2856–2860
35. Cox, J., Matic, I., Hilger, M., Nagaraj, N., Selbach, M., Olsen, J. V., and Mann, M. (2009) A practical guide to the MaxQuant computational platform for SILAC-based quantitative proteomics. *Nat. Protoc.* **4,** 698–705
36. Sandberg, R., and Larsson, O. (2007) Improved precision and accuracy for microarrays using updated probe set definitions. *BMC Bioinformatics* **8,** 48
37. Smyth, G. (2005) Limma: linear models for microarray data; Bioinformatics and computational biology solutions using R and Bioconductor, **23,** 397–420
38. Kimmel, C. B., Ballard, W. W., Kimmel, S. R., Ullmann, B., and Schilling, T. F. (1995) Stages of embryonic development of the zebrafish. *Dev. Dyn.* **203,** 253–310
39. Geiger, T., Cox, J., Ostasiewicz, P., Wisniewski, J. R., and Mann, M. (2010) Super-SILAC mix for quantitative proteomics of human tumor tissue. *Nat. Methods* **7,** 383–385
40. Diekmann, H., and Stuermer, C. A. (2009) Zebrafish neurolin-a and -b, orthologs of ALCAM, are involved in retinal ganglion cell differentiation and retinal axon pathfinding. *J. Comp. Neurol.* **513,** 38–50
41. Choudhry, P., Joshi, D., Funke, B., and Trede, N. (2011) Alcama mediates Edn1 signaling during zebrafish cartilage morphogenesis. *Dev. Biol.* **349**, 483–493
42. Zimmerman, A. W., Nelissen, J. M., van Emst-de Vries, S. E., Willems, P. H., de Lange, F., Collard, J. G., van Leeuwen, F. N., and Figdor, C. G. (2004) Cytoskeletal restraints regulate homotypic ALCAM-mediated adhesion through PKCα independently of Rho-like GTPases. *J. Cell Sci.* **117,** 2841–2852
43. Arstikaitis, P., Gauthier-Campbell, C., Carolina Gutierrez Herrera, R., Huang, K., Levinson, J. N., Murphy, T. H., Kilimann, M. W., Sala, C., Colicos, M. A., and El-Husseini, A. (2008) Paralemmin-1, a modulator of filopodia induction is required for spine maturation. *Mol. Biol. Cell* **19,** 2026–2038
44. Lieschke, G. J., and Currie, P. D. (2007) Animal models of human disease: zebrafish swim into view. *Nat. Rev. Genet.* **8,** 353–367
45. Ofori-Acquah, S. F., and King, J. A. (2008) Activated leukocyte cell adhesion molecule: a new paradox in cancer. *Transl. Res.* **151,** 122–128
46. Hirata, H., Murakami, Y., Miyamoto, Y., Tosaka, M., Inoue, K., Nagahashi, A., Jakt, L. M., Asahara, T., Iwata, H., Sawa, Y., and Kawamata, S. (2006) ALCAM (CD166) is a surface marker for early murine cardiomyocytes. *Cells Tissues Organs* **184,** 172–180
47. Carroll, D. (2011) Genome engineering with zinc-finger nucleases. *Genetics* **188,** 773–782
48. Boch, J., Scholze, H., Schornack, S., Landgraf, A., Hahn, S., Kay, S., Lahaye, T., Nickstadt, A., and Bonas, U. (2009) Breaking the code of DNA binding specificity of TAL-type III effectors. *Science* **326,** 1509–1512